

## Inhibition, dispersion and corrosion performance of a novel modified polyepoxysuccinic acid

Yiyi Chen<sup>a</sup>, Yuming Zhou<sup>a,b,\*</sup>, Qingzhao Yao<sup>a,\*</sup>, Qiuli Nan<sup>b</sup>, Mingjue Zhang<sup>b</sup>, Wei Sun<sup>c</sup>

<sup>a</sup>School of Chemistry and Chemical Engineering, Southeast University, Nanjing 211189, China, Tel. +86 25 52090617; emails: ymzhou@seu.edu.cn (Y. Zhou), 101006377@seu.edu.cn (Q. Yao), chenyyiyi0220@126.com (Y. Chen)

<sup>b</sup>School of Pharmaceutical and Chemical Engineering, Chengxian College, Southeast University, Nanjing, Jiangsu Province, 210088, China, Tel. +86 25 52090617; emails: 53212651@qq.com (Q. Nan), 489354839@qq.com (M. Zhang)

<sup>c</sup>Jianghai Environmental Protection Co. Ltd., Changzhou 213116, China, Tel. +86 25 52090617; email: leojhgh@sina.com

Received 5 March 2019; Accepted 29 June 2019

### ABSTRACT

A novel modified polyepoxysuccinic acid polymer, epoxysuccinic acid-oxalic acid-allylpolyethoxy carboxylate (ESA-co-APEM, PEM), was prepared through free-radical polymerization reaction of ESA and APEM and characterized by Fourier transform infrared spectroscopy. The polymer's ability to inhibit calcium sulfate scale formation, disperse ferric oxide is investigated by static tests and its corrosion inhibition performance was studied via weight loss measurements. The scale inhibition efficiency of CaSO<sub>4</sub> could reach 99% in the concentration of 4 mg/L, the best dispersion efficiency was reached to 20% (transmittance) when 18 mg/L of PEM was used, and the corrosion inhibition efficiency increased to 70% when the concentration was 60 mg/L. Scanning electron microscopy was used to analyze the effects of PEM on morphology of calcium sulfate and corrosion inhibition of carbon steel. The results showed that PEM possessed outstanding ability of inhibition, dispersion and corrosion inhibition properties.

*Keywords:* Modified polyepoxysuccinic acid; Calcium sulfate inhibition; Fe<sub>2</sub>O<sub>3</sub> dispersion; Corrosion inhibition

### 1. Introduction

Recirculating cooling water systems are frequently utilized in manufacturing facilities due to the severe shortage of the water resource supply. During circulation process, the substances present in the thermal fluid can accumulate and become concentrated with water evaporating and increasing temperature. This will cause the formation of scales, among which calcium sulfate is common in circulating system and always attach to the surface of equipment, causing heat transfer blocking and the flow rate reducing [1–3]. Therefore, a technique is required for quick and effective scales elimination such as inhibitors added in recycling water treatment systems.

In cooling water systems, iron-based compounds from feed water, such as FeCl<sub>3</sub> and Fe<sub>2</sub>(SO<sub>4</sub>)<sub>3</sub>, are main sources of iron element. The ferric ion is unstable and will encounter hydrolysis to form insoluble hydroxides, which can precipitate on the surface of heat exchanger and lead to corrosion of pipes. Fe<sup>2+</sup>, lower valency of iron, is soluble and poses no threat to solutions. Thus, with the increasing of pH values and touching air, the ferrous ion will be oxidized to ferric ion. On the other hand, the existence of iron compounds can affect the inhibition performance of scale inhibitors, such as polymers of acrylic acids [4–6]. Supreme scale inhibitors should also be effective for dispersing the iron compounds accordingly.

\* Corresponding authors.

Corrosion is another problem resulting from using water as thermal fluids because the qualities of equipments and facilities are mainly carbon steels and stainless steels [7]. Carbon steel, as is known, is easy to corrode under many circumstances, especially the process of chemical cleaning with the use of acids. This process is both costly and dangerous which will cause deterioration of metallic equipment at the external or internal surface of a material. Then the great economic loss and catastrophic accidents will happen. Corrosion inhibitor, a chemical substance, is useful to decrease the corrosion rate of metals. Hence, developing non-toxic, biodegradable, relatively cheap and completely soluble inhibitor for corrosion is imminent [8–10].

Phosphate groups, sulfonate groups and carboxylic groups are three groups of common polymeric scale inhibitors. Polymers containing phosphate groups can hydrolyze to useless orthophosphate and then form calcium phosphate scales in the presence of calcium ions, which will be possible to accelerate water eutrophication and run counter to the goal of environment protection [11,12]. Polymers with sulfonate groups display poor performance in certain conditions, such as high temperature, high hardness and high pH. While polymers containing carboxylic groups also have disadvantages such as low calcium tolerance and can produce insolubilization of unexpected complexes with excessive amounts of calcium ions [13,14]. As a result, the development of biodegradable inhibitors being friendly to the environment that exhibit outstanding performance in water treatment can be promising.

Polyepoxysuccinic acid (PESA), which has carboxyl and ether groups in its molecular chain, is considered a biodegradable and environmental friendly polymer. Polyepoxysuccinic acid is also a good substitute for conventional scale inhibitors because it exhibits excellent dispersion performance of  $\text{Fe}_2\text{O}_3$ . As a result, PESA has been paid considerable attention from researchers all over the world [15–17]. According to literature, this polymer was proved to chelate  $\text{Ca}^{2+}$  by forming water-soluble complexes in water, so then the deposition of calcium salts could be reduced. And PESA has also exhibited good corrosion inhibition ability of carbon steel in acid environment. For high-hardness systems, PESA is especially suitable, such as membrane separation, boiler water treatment, circulating cooling water treatment [16]. However, its overall properties are poor, and this limits its use. Therefore, for the sake of enhancing its comprehensive performance, the introduction of functional groups on the side chains was conformed to be the most effective [18].

Herein, a modified and new polyepoxysuccinic acid inhibitor (PEM) was designed with epoxysuccinic acid (ESA)

and oxalic acid-allylpolyethoxy carboxylate (APEM), which was a new type of inhibitor to inhibit calcium sulfate scale, disperse ferric oxide and inhibit carbon steel corrosion. Fourier transform infrared spectroscopy (FT-IR) was used to characterize PEM. The scale inhibition performance and its ability to disperse  $\text{Fe}_2\text{O}_3$  of PEM were studied by static scale inhibition test, while the corrosion inhibition performance by PEM was examined through weight loss measurements. To further study the scale and corrosion inhibition mechanism of PEM, the morphology and structure of calcium sulfate scale and carbon steel were observed by scanning electron microscopy (SEM).

## 2. Experimental

### 2.1. Reagents

Maleic anhydride, hydrogen peroxide, sodium tungstate, calcium chloride, sodium sulfate, ferric chloride, sodium hydrate, sodium bicarbonate, bitter salts, sodium chloride and hydrochloric acid were obtained from Zhongdong Chemical Reagent Co. Ltd. (Nanjing, Jiangsu, People's Republic of China). All the above chemicals were in analytically pure grade without further purification, unless otherwise specified. Deionized water was used throughout the experiment.

### 2.2. Preparation of PEM

#### 2.2.1. Synthesis of ESA

9.8 g (0.1 mol) of maleic anhydride was dissolved in 20 mL deionized water in a three-neck flask under alkaline conditions. Then 20 mL of hydrogen peroxide was slowly added into it, and reacted at 50°C for 1.5 h with magnetic stirring. After that, the solution was separated with ethyl alcohol and dried under nitrogen to 90°C. The synthesis procedure of ESA is shown in Fig. 1.

#### 2.2.2. Synthesis of APEM

APEM was synthesized in our laboratory according to our previous studies [19]. Allyloxy polyethoxy ether (APEG) was carboxylate terminated using oxalic acid with a molar ratio of 1:1. Synthesis procedure of APEM is shown in Fig. 2.

#### 2.2.3. Synthesis of PEM

PEM was synthesized by ESA, APEM as monomers and ammonium persulfate as initiator. A definite proportion of ESA and APEM (the mole ratio of ESA to APEM was 2:1)

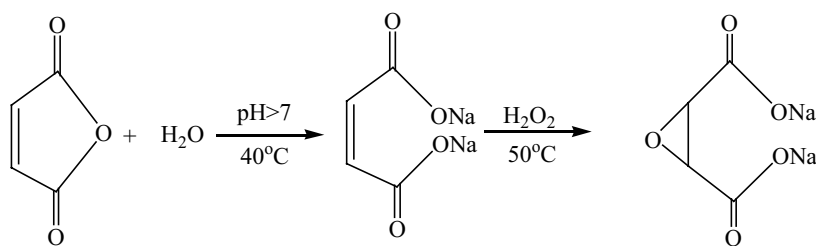


Fig. 1. Preparation of ESA.

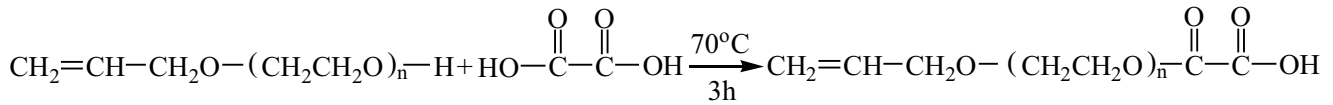


Fig. 2. Preparation of APEM.

was dissolved in deionized water in a three-neck flask and heated to the reaction temperature 70°C over a period of time under nitrogen atmosphere. Then, a certain amount of the ammonium persulfate solution was slowly dropped into the three-neck flask mentioned above. At last, the modified biodegradable polymer PEM was obtained, containing about 20.34% solid. The synthesis procedure of is shown in Fig. 3.

The products were characterized with IR spectra. About 1 mg dried PEM was mixed with 100 mg dried KBr powder and then compressed into a disk for spectrum recording at room temperature.

2.3. Methods for evaluation of calcium sulfate scale inhibition, ferric oxide dispersion and carbon steel corrosion inhibition by PEM

2.3.1. Static tests for CaSO<sub>4</sub> scale inhibition

The scale inhibition performance of the prepared polymer against calcium sulfate was investigated by static scale inhibition tests according to the Chinese National Standard concerning the code for the design of industrial oil field-water treatments (SY/T 5673-93). The solution in calcium sulfate inhibition tests contained CaCl<sub>2</sub> (6,800 mg/L Ca<sup>2+</sup>),

Na<sub>2</sub>SO<sub>4</sub> (7,100 mg/L of SO<sub>4</sub><sup>2-</sup>) and different concentration of polymers, which then was heated in a water bath at 60°C for 6 h. The Ca<sup>2+</sup> concentrations of all of those solutions were titrated by 0.05 mg/L sodium ethylene diamine tetraacetate standard solution. The inhibition efficiency η was defined as follows:

$$\eta = \frac{\rho_1(\text{Ca}^{2+}) - \rho_2(\text{Ca}^{2+})}{\rho_0(\text{Ca}^{2+}) - \rho_2(\text{Ca}^{2+})} \times 100\% \quad (1)$$

where ρ<sub>0</sub> (Ca<sup>2+</sup>) is the total concentrations of Ca<sup>2+</sup> (mg/L), ρ<sub>1</sub> (Ca<sup>2+</sup>) is the concentrations of Ca<sup>2+</sup> (mg/L) in the presence of the polymer inhibitor, ρ<sub>2</sub> (Ca<sup>2+</sup>) is the concentrations of Ca<sup>2+</sup> (mg/L) in the absence of the polymer inhibitor.

2.3.2. Static tests for ferric oxide dispersion

The iron dispersion properties of the polymer PEM was tested through UV-visible studies. Ferrous compounds for the experiment were prepared by adding a known volume of calcium stock solution and iron (II) stock solution to a beaker (1,000 mL) with a certain amount of deionized

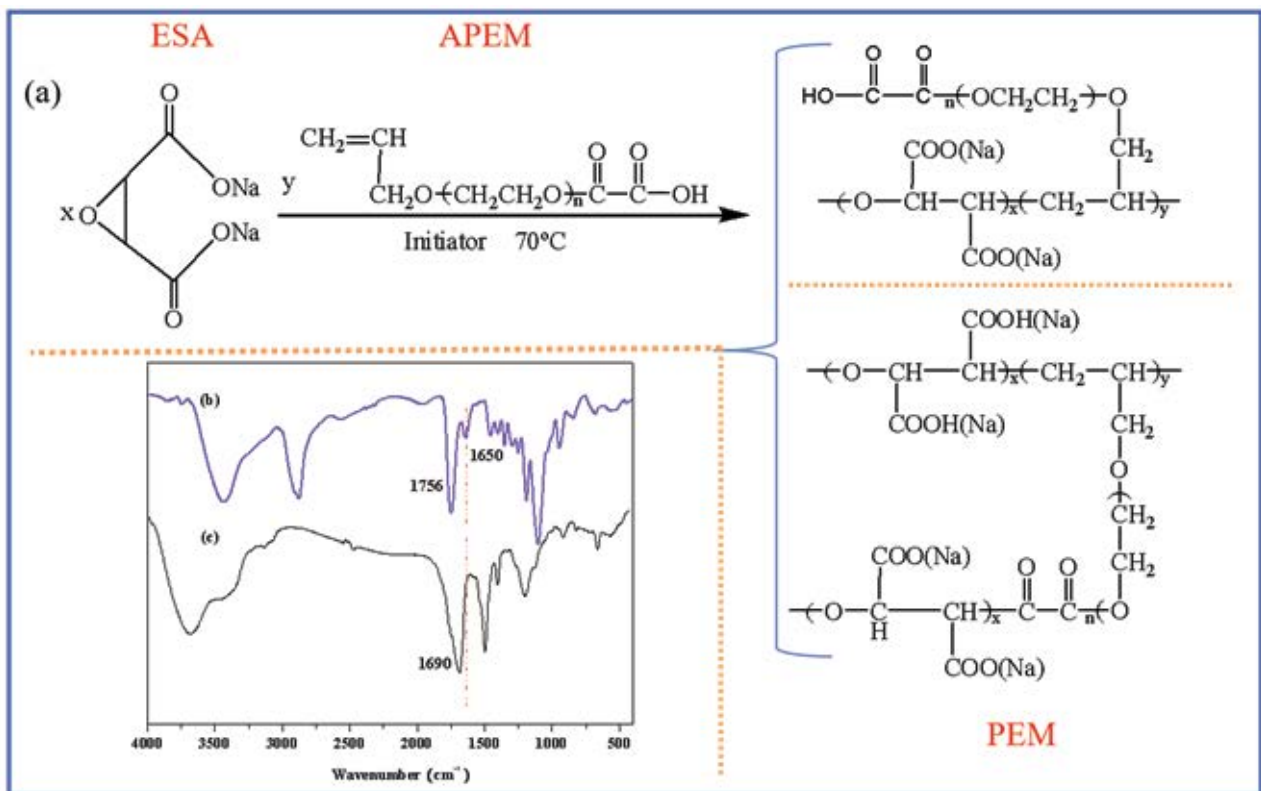


Fig. 3. (a) Preparation of PEM, (b) FT-IR spectra of APEM and (c) FT-IR spectra of PEM.

water at room temperature under continuous stirring. The mixed solution contained 150 mg/L  $\text{Ca}^{2+}$  and 10 mg/L  $\text{Fe}^{2+}$ . Then the pH value of the solution was adjusted to 9.0 with borax and the solution was evenly mixed with a known amount of PEM polymer. Mixed solution was stirred for 15 min and heated at 50°C for 5 h before being cooled to room temperature. After that, the dispersion performance was evaluated under the wavelength of 420 nm with 722-spectrophotometer by light transmittance.

### 2.3.3. Weight loss measurement

According to the China National Standard GB/T 18175-2000, the corrosion inhibition efficiency of PEM polymer was measured by weight loss measurement of rotating hung steel slices. The surface area of tested low carbon steel is 28.00  $\text{cm}^2$  and its chemical composition is listed as follows: 0.17%–0.23% C, 0.17%–0.37% Si, 0.35%–0.65% Mn,  $\leq 0.25\%$  Cr,  $\leq 0.3\%$  Ni,  $\leq 0.25\%$  Cu, and balance Fe. The weight loss of steel coupons was evaluated after these were immersed in the prepared solutions which are open to the atmosphere at a constant temperature of 45°C for 72.0 h. Every 4 h, a certain amount of distilled water was added in the solutions. The corrosion efficiency was calculated by Eqs. (2) and (3) as follows:

$$X = \frac{87,600 \times [(m_0 - m_1) - \Delta m]}{s \times \rho \times t} \quad (2)$$

$$\eta = \frac{X_0 - X_1}{X_0} \times 100\% \quad (3)$$

where  $m_0$  is the mass of carbon steel hung slices before test;  $m_1$  is the mass of carbon steel hung slices after test;  $\Delta m$  is the mass loss of carbon steel hung slices caused by washing in acid (20% HCl and 8 g/L of aminoform).  $s$  is the surface area of carbon steel hung slice (28  $\text{cm}^2$ ).  $t$  is the testing time (72 h).  $\rho$  is the density of carbon steel hung slices.  $X_0$  is the annual corrosion rate in the absence of scale inhibitor (mm/year).  $X_1$  is the annual corrosion rate in the presence of scale inhibitor (mm/y).  $\eta$  is the corrosion inhibition efficiency (%).

### 2.4. Morphology characterization

The morphological change of the  $\text{CaSO}_4$  crystals and carbon steel on glass plates was examined through SEM, with the addition of the polymer PEM. The samples were coated with a layer of gold and observed in an S-3400N Hi-TECH (Taiwan, China) SEM. Also the crystal changes of  $\text{CaSO}_4$  were studied by X-ray diffraction (XRD).

## 3. Results and discussion

### 3.1. Characterizations

The FT-IR spectra of ESA, APEM and PEM are exhibited in Figs. 4, 3b and 3c. As can be seen from curve of ESA that the characteristic absorption peaks at 850, 945 and 1,230  $\text{cm}^{-1}$  are attributed to C–O–C closed loop, deformation vibration, symmetrical stretching vibration and asymmetric stretching

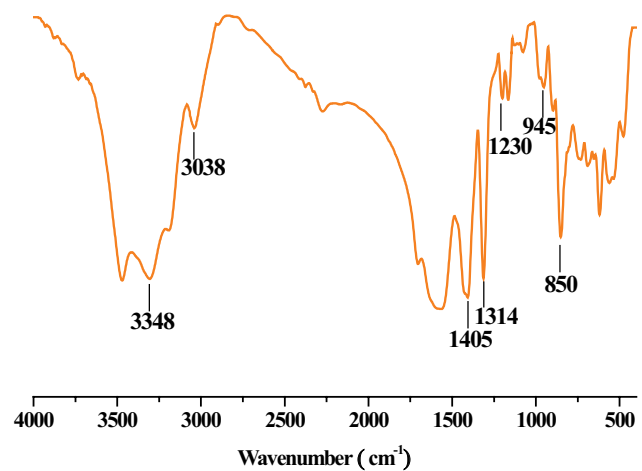


Fig. 4. FT-IR spectra of ESA.

vibration for each. The forming of C–O–C closed loop means the forming of designed targeted functional groups, a three-membered ring epoxy structure. Other characteristic peaks of ESA have also appeared: 1,314; 1,405; 3,038 and 3,348  $\text{cm}^{-1}$ , corresponding to vibration of C–H, O–H, C–H (methenyl) and O–H, respectively. In the curve of APEM, the C=C absorption peak appears at 1,650  $\text{cm}^{-1}$ , and there are no peaks between 1,620 and 1,680  $\text{cm}^{-1}$  in curve of PEM. Meanwhile, the fact that the cycle C–O–C bond stretching vibration at 1,128  $\text{cm}^{-1}$  appears but the absorption peaks at 3,038; 1,230 and 945  $\text{cm}^{-1}$  disappear completely reveals that the polymerization reaction has taken place between the reaction monomers and PEM has been synthesized.

### 3.2. Calcium sulfate scale inhibition performance by PEM

#### 3.2.1. Effects of PEM dosages

Compared with commercial inhibitors, the effect of PEM with different dosages on scale inhibition efficiency against  $\text{CaSO}_4$  is researched in Fig. 5. For PEM, the results indicate that the scale inhibition efficiency obviously increases with increasing the concentration of PEM before the dosage of 4 mg/L and slightly increases when the concentration is over 4 mg/L, exhibiting an obvious threshold effect. And the scale inhibition efficiency can reach 99% in the concentration of 4 mg/L, indicating that PEM has good ability against  $\text{CaSO}_4$ .

On the other hand, PEM also shows much better inhibition efficiency than ATMP, PESA, PAA, HPMA and PBTCA. The best inhibition efficiency of PESA reached approximately 86.8%; while the inhibition efficiencies of ATMP, PAA, HPMA and PBTCA reached 86.3%, 80.4%, 79.5% and 67.4%, respectively. This may put down to the multifunctional groups with negative charge in PEM molecule, which have strong adsorption to calcium sulfate microcrystal and occupy the active growth point of calcium sulfate crystal. At last, the normal growth may be ruined, and then prevent the generation of  $\text{CaSO}_4$  scale.

#### 3.2.2. Influence of solution property

Specific effects, solution property, such as  $\text{Ca}^{2+}$  concentration, change of pH and temperature have great influence

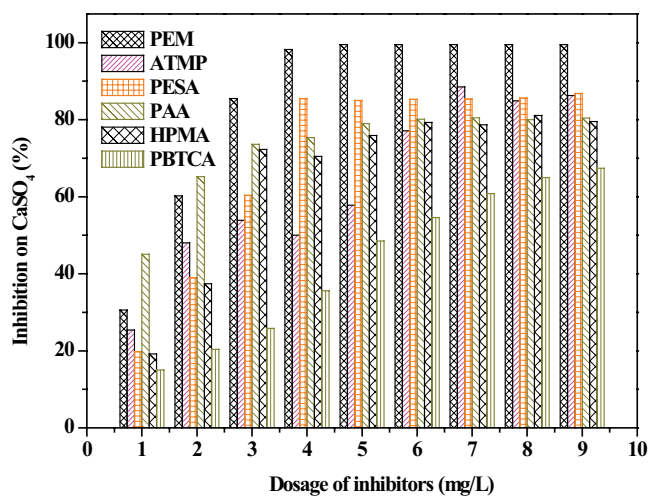


Fig. 5. Inhibition performance of PEM against CaSO<sub>4</sub>.

on scale inhibition performance. As shown in Fig. 6, effect of change in concentration of Ca<sup>2+</sup> from 6,800 to 20,400 mg/L was tested. The data show that the scale inhibition efficiency against CaSO<sub>4</sub> decreases with increasing Ca<sup>2+</sup> concentration, while the efficiency is still close to 80% when Ca<sup>2+</sup> concentration increases to 20,400 mg/L, which means PEM could be used in high hardness water solution.

Temperature is another essential factor on scale inhibition performance as shown in Fig. 7. The Ca<sup>2+</sup> concentration is 6,800 mg/L, the concentration of PEM is 4 mg/L, the temperature is in the range of 50°C–90°C and pH value is 7. It is apparent that scale inhibition efficiency decreases with rising water temperature, and the scale inhibition efficiency is above 80% when it is 90°C, indicating that PEM is suitable for water in high temperature.

Fig. 8 displays the influence of solution pH values on calcium sulfate scale inhibition performance. The Ca<sup>2+</sup> concentration is 6,800 mg/L, the concentration of PEM is 4 mg/L, the temperature is 60°C. When the pH increases from 7 to 9, the scale inhibition efficiency decreases from 98.2% to 82.4%. The increasing pH value will break up the equilibrium between Ca<sup>2+</sup> and SO<sub>4</sub><sup>2-</sup>, and promote the formation of calcium sulfate.

### 3.2.3. SEM and XRD characterization of CaSO<sub>4</sub>

The scale inhibition mechanism of PEM was further investigated by directly observing the surface morphology of precipitated CaSO<sub>4</sub> scales by using SEM, as shown in Fig. 9 (in the absence and presence of PEM). Fig. 9a shows the blank calcium sulfate crystals having regular shape similar to a slim needle and a smooth surface. When PEM is added, the original shape of the calcium sulfate crystals is destroyed and the crystals become more and more loose. Plate-shaped particles have appeared and are easily removed with flowing water.

Fig. 10 exhibits the XRD spectra of calcium sulfate crystals without and with the addition of PEM. Without addition of inhibitor, diffraction peaks appeared at 11.66°, 20.71°, 23.34° and 29.40° are characteristic peaks of calcium sulfate crystals, while the peaks have little changes with the addition

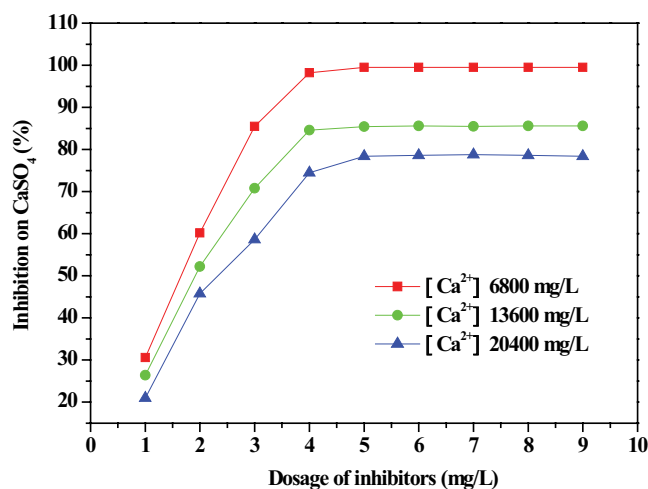


Fig. 6. Effects of Ca<sup>2+</sup> concentration on inhibition performance of PEM against CaSO<sub>4</sub>.

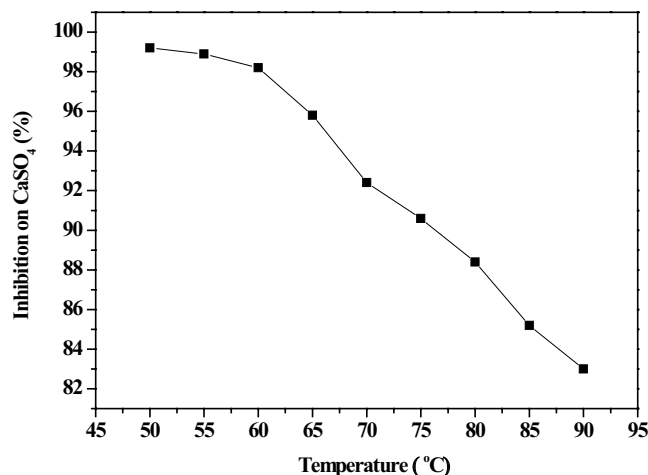


Fig. 7. Effects of temperature on inhibition performance of PEM against CaSO<sub>4</sub>.

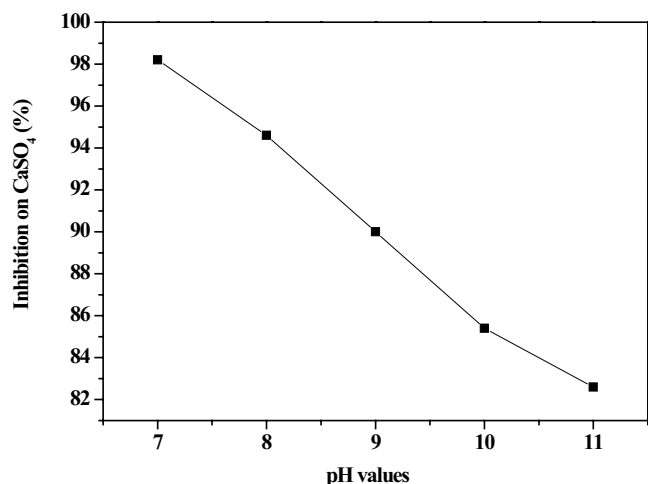


Fig. 8. Effects of pH values on inhibition performance of PEM against CaSO<sub>4</sub>.

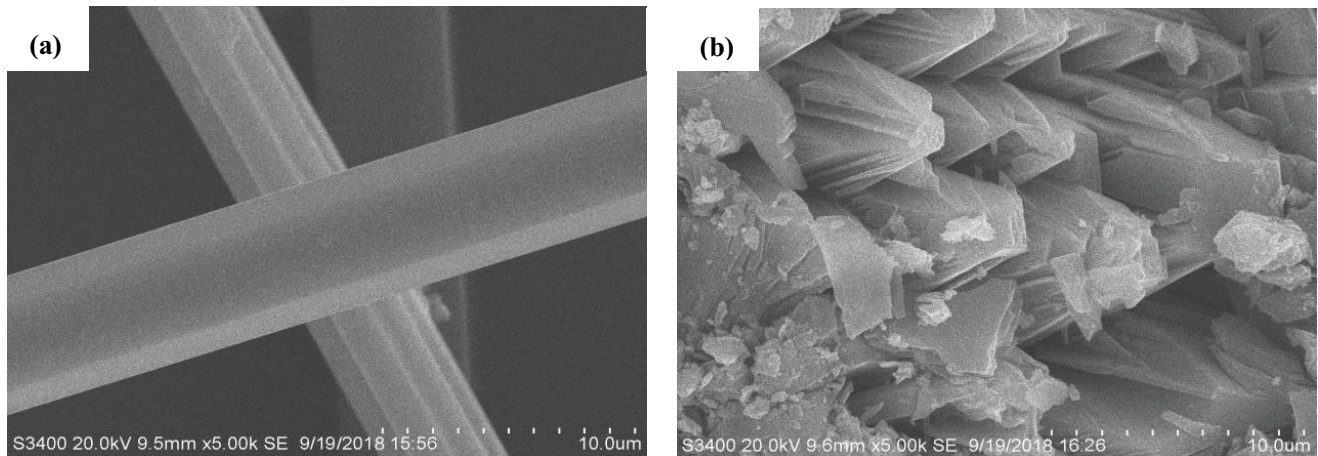


Fig. 9. SEM images of  $\text{CaSO}_4$  (a) in the absence of PEM and (b) in the presence of 4 mg/L PEM.

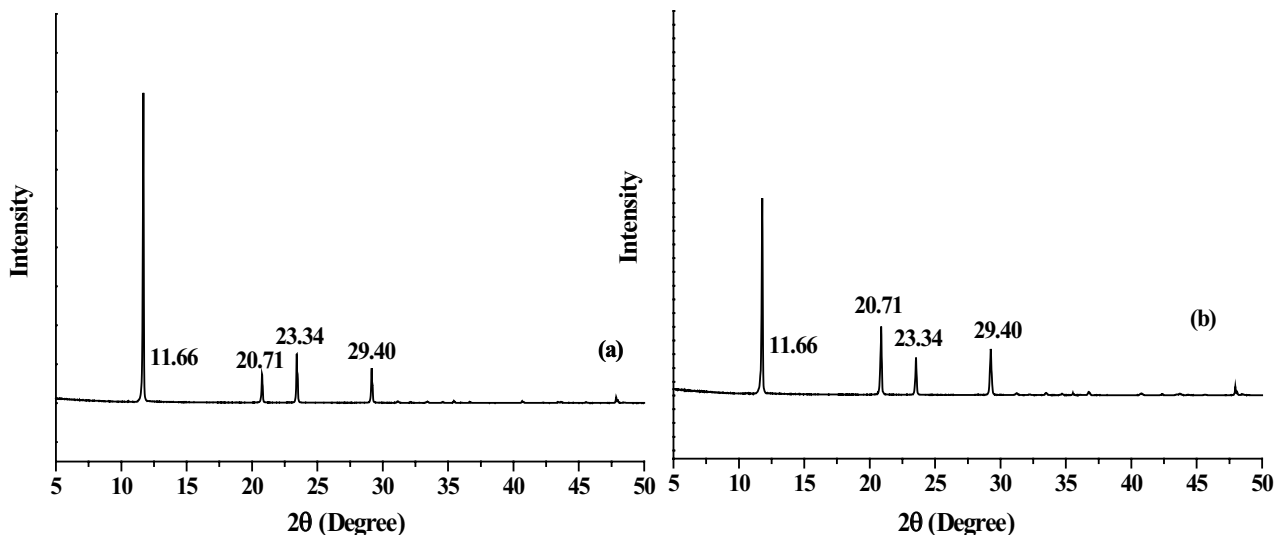


Fig. 10. XRD spectrum of  $\text{CaSO}_4$  (a) in the absence of PEM and (b) in the presence of 4 mg/L PEM.

of PEM, as shown in spectrum (b). The results indicate that the presence of PEM can only change the surface morphology and particle size.

### 3.3. $\text{Fe}_2\text{O}_3$ dispersion performance of PEM

The dispersion performance of PEM is shown in Fig. 11, comparing with HPMA (a commonly used polyacrylic acid derivative inhibitor) and PESA (having similar structure with PEM). HPMA and PESA exhibit hardly any ability to disperse ferric oxide, whereas PEM possesses excellent dispersion ability. In the experimental conditions, it is disclosed that the transmittance ratio to disperse ferric oxide reduces along with the increase of PEM dosage from 0 to 18 mg/L and the best dispersion efficiency is reached to 20% (transmittance) when 18 mg/L of PEM is added into the tested solution. According to this result, the PEG groups on PEM matrix play an important role on dispersion to ferric oxide. The mechanism is the adsorption of the lone pair electrons in the PEG groups to the surfaces of ferric oxide

crystal particles through electrostatic interactions, which will lead to uniformly dispersed ferric oxide in water, as shown in Fig. 12.

### 3.4. Corrosion inhibition performance of PEM

The effect of PEM dosages on corrosion inhibition performance is shown in Fig. 13, comparing with EDTMP and PESA, commercial and commonly used corrosion inhibitors. According to the data, PEM has excellent ability on the corrosion inhibition, because the efficiency increases to 70% when the concentration is 60 mg/L while the efficiency of EDTMP is only 35% at this concentration. Although PESA has superior ability to inhibit calcium carbonate, its corrosion ability for carbon steel is poor. When the concentration is 80 mg/L, its corrosion inhibition performance is only 25%.

The surface morphology of carbon steel in the absence and presence of PEM was observed by photos and SEM in Fig. 14. Figs. 14a and d show that carbon steel seems very rough on the surface and is considerably damaged without

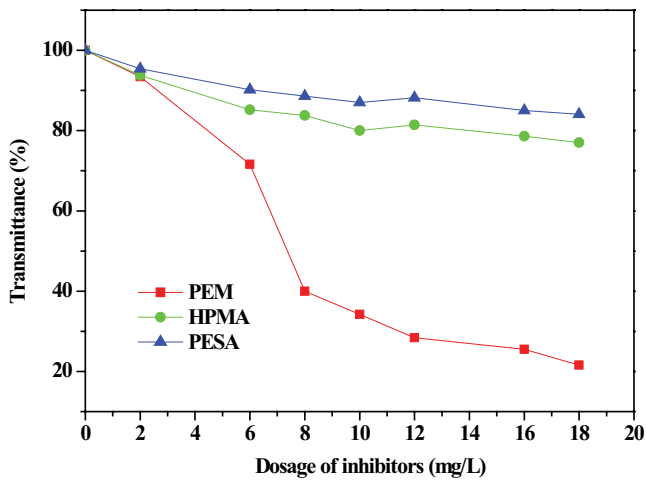


Fig. 11. Fe<sub>2</sub>O<sub>3</sub> dispersion performance of PEM.

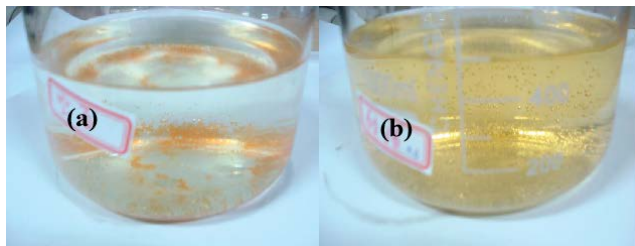


Fig. 12. Photographs of effects of Fe<sub>2</sub>O<sub>3</sub> dispersion performance of PEM.

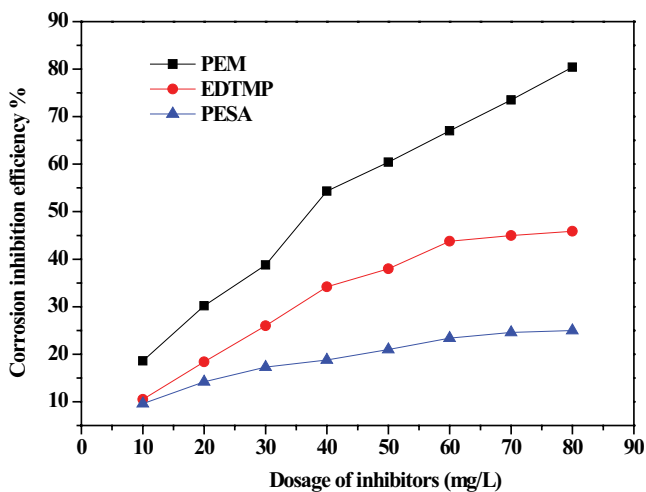


Fig. 13. Corrosion inhibition efficiency of PEM.

PEM, while the rough surface becomes better and better with the increase in concentration of inhibitor, as is apparent in Figs. 14b and c. The change can also be seen from Fig. 14e, as the surface gets smooth. These results illustrate that PEM has a good performance in protecting the carbon steel from corrosion.

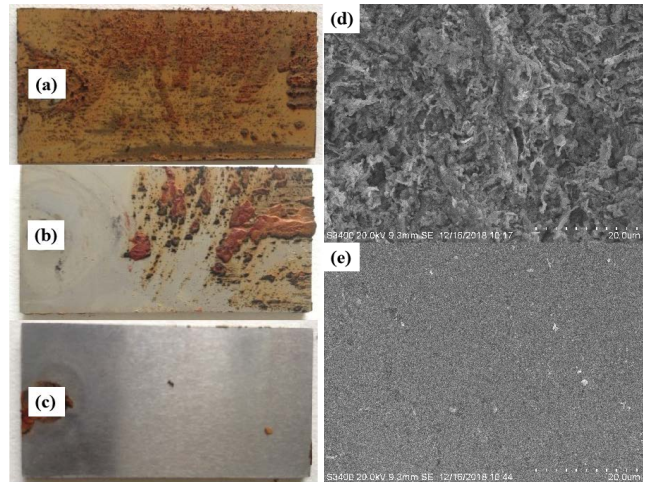


Fig. 14. Photographs and SEM images of corrosion inhibition effects of PEM, (a, d) without PEM; (b) with 40 mg/L of PEM; (c, e) with 80 mg/L of PEM.

#### 4. Conclusion

The present work constructed a new modified poly-epoxysuccinic acid scale and corrosion inhibitor (PEM) by the free-radical polymerization reaction. PEM is proven to be an effective inhibitor by performance tests with calcium sulfate scale inhibition efficiency of 99% in the concentration of 4 mg/L and dispersion efficiency of 20% for Fe<sub>2</sub>O<sub>3</sub> at the dosage of 18 mg/L. Meanwhile, the corrosion inhibition efficiency is 70% at the concentration of 60 mg/L. A certain theoretical and experimental support for PEM is provided and it will be a novel and potential material for inhibition of scale and corrosion, and dispersion.

#### Acknowledgments

This work was supported by the National Natural Science Foundation of China (51673040), the Natural Science Foundation of Jiangsu Province (BK20171357), the Fundamental Research Funds for the Central Universities (2242018k30008, 3207048418), Scientific Innovation Research Foundation of College Graduate in Jiangsu Province (KYLX16\_0266, KYCX17\_0134), a Project Funded by the Priority Academic Program Development of Jiangsu Higher Education Institutions (PADA) (1107047002), Fund Project for Transformation of Scientific and Technological Achievements of Jiangsu Province of China (BA2016105) and Young Teachers' Research Development Fund of Southeast University Chengxian College (z0016, 2019). Based on scientific research SRTP of Southeast University (T16192020), and the Scientific Research Foundation of Graduate School of Southeast University (YBJJ1417).

#### References

- [1] Z. Shen, X. Zhi, P. Zhang, Preparation of fluorescent polyaspartic acid and evaluation of its scale inhibition for CaCO<sub>3</sub> and CaSO<sub>4</sub>, *Polym. Adv. Technol.*, 28 (2017) 367–372.
- [2] S.C. Shi, D.Y. Li, C.X. Chai, Y.F. Wu, Y. Xu, Synthesis of a polyaspartic acid/4-(2-aminoethyl) morpholine graft copolymer

- and evaluation of its scale and corrosion inhibition performance, *Polym. Adv. Technol.*, 29 (2018) 2838–2847.
- [3] J. Li, Y.M. Zhou, Q.Z. Yao, T.T. Wang, A. Zhang, Y.Y. Chen, W.D. Wu, W. Sun, Preparation and evaluation of a polyether-based polycarboxylate as a kind of inhibitor for water systems, *Ind. Eng. Chem. Res.*, 56 (2017) 2624–2633.
- [4] C.E. Fu, Y.M. Zhou, J.Y. Huang, H.T. Xie, G.Q. Liu, W.D. Wu, W. Sun, Control of iron(III) scaling in industrial cooling water systems by the use of maleic anhydride-ammonium allylpolyethoxy sulphate dispersant, *Adsorpt. Sci. Technol.*, 28 (2010) 437–448.
- [5] C.E. Fu, Y.M. Zhou, H.T. Xie, W. Sun, W.D. Wu, Double-hydrophilic block copolymers as precipitation inhibitors for calcium phosphate and iron(III), *Ind. Eng. Chem. Res.*, 49 (2010) 8920–8926.
- [6] R. Ketrane, B. Saidani, O. Gil, L. Leleyter, F. Baraud, Efficiency of five scale inhibitors on calcium carbonate precipitation from hard water: effect of temperature and concentration, *Desalination*, 249 (2009) 1397–1404.
- [7] R. Touira, N. Dkhirechea, M. Ebn Touhami, M. Sfaira, O. Senhaji, J.J. Robin, B. Boutevin, M. Cherkaoui, Study of phosphonate addition and hydrodynamic conditions on ordinary steel corrosion inhibition in simulated cooling water, *Mater. Chem. Phys.*, 122 (2010) 1–9.
- [8] M.A. Migahed, S.M. Rashwan, M.M. Kamel, R.E. Habib, Synthesis, characterization of polyaspartic acid-glycine adduct and evaluation of their performance as scale and corrosion inhibitor in desalination water plants, *J. Mol. Liq.*, 224 (2016) 849–858.
- [9] M. Gopiraman, N. Selvakumaran, D. Kesavan, I.S. Kim, R. Karvembu, Chemical and physical interactions of 1-benzoyl-3, 3-disubstituted thiourea derivatives on mild steel surface: corrosion inhibition in acidic media, *Ind. Eng. Chem. Res.*, 51 (2012) 7910–7922.
- [10] T.T. Wang, Y.M. Zhou, Q.Z. Yao, J. Li, A. Zhang, Y.Y. Chen, X.N. Chen, Q.L. Nan, M.J. Zhang, W.D. Wu, W. Sun, Synthesis of double-hydrophilic antiscalant and evaluation of its  $\text{CaCO}_3$ ,  $\text{CaSO}_4$  and  $\text{Ca}_3(\text{PO}_4)_2$  precipitation performance, *Desal. Wat. Treat.*, 78 (2017) 107–116.
- [11] F.H. Butt, F. Rahman, U. Baduruthamal, Identification of scale deposits through membrane autopsy, *Desalination*, 101 (1995) 219–230.
- [12] Z. Amjad, Investigations on the evaluation of polymeric calcium sulfate dihydrate (gypsum) scale inhibitors in the presence of phosphonates, *Desal. Wat. Treat.*, 37 (2012) 268–276.
- [13] M. Pérez-Alvarez, R. Oviedo-Roa, E. Soto-Castruita, E. Buenrostro-González, R. Cisneros-Dévora, D. Nieto-Álvarez, M. Pons-Jiménez, L.S. Zamudio-Rivera, Growth inhibition in calcium sulfate crystal using a copolymer in oil fields: theoretical study and experimental evaluations, *Iran. Polym. J.*, 27 (2018) 927–937.
- [14] Y.Y. Chen, Y.M. Zhou, Q.Z. Yao, Y.Y. Bu, H.C. Wang, W.D. Wu, W. Sun, Preparation of a low-phosphorous terpolymer as a scale, corrosion inhibitor, and dispersant for ferric oxide, *J. Appl. Polym. Sci.*, 132 (2015) 1–7.
- [15] W.Y. Shi, W. Xu, H. Cang, X.H. Yan, R. Shao, Y.H. Zhang, M.Z. Xia, Design and synthesis of biodegradable antiscalant based on MD simulation of antiscalant mechanism: a case of itaconic acid-epoxysuccinate copolymer, *Comp. Mater. Sci.*, 136 (2017) 118–125.
- [16] M. Chaussemier, E. Pourmohtasham, D. Gelus, State of art of natural inhibitors of calcium carbonate scaling, *Desalination*, 356 (2015) 47–55.
- [17] X.H. Zhou, Y.H. Sun, Y.Z. Wang, Inhibition and dispersion of polyepoxysuccinate as a scale inhibitor, *J. Environ. Sci.*, 23 (Supplement) 2011 S159–S161.
- [18] A. Zhang, Y.M. Zhou, Q.Z. Yao, T.T. Wang, J. Li, Y.Y. Chen, Q.L. Nan, M.J. Zhang, W.D. Wu, W. Sun, Inhibition of calcium carbonate and sulfate scales by a polyether-based polycarboxylate antiscalant for cooling water systems, *Desal. Wat. Treat.*, 77 (2017) 306–314.
- [19] Y.Y. Chen, Y.M. Zhou, Q.Z. Yao, Y.Y. Bu, H.C. Wang, W.D. Wu, W. Sun, Evaluation of a low-phosphorus terpolymer as calcium scales inhibitor in cooling water, *Desal. Wat. Treat.*, 18 (2015) 945–955.